Effects of monomer functionality on performances of scaffolding morphologic transmission gratings recorded in polymer dispersed liquid crystals

2015 J. Phys. D: Appl. Phys. 48 375303

(http://iopscience.iop.org/0022-3727/48/37/375303)

IOP Publishing Journal of Physics D: Applied Physics
J. Phys. D: Appl. Phys. **48** (2015) 375303 (9pp) doi:10.1088/0022-3727/48/37/375303

Effects of monomer functionality on performances of scaffolding morphologic transmission gratings recorded in polymer dispersed liquid crystals

Wenbin Huang[1,2], Donglin Pu[1,2], Su Shen[1,2], Guojun Wei[1,2], Li Xuan[3] and Linsen Chen[1,2]

[1] College of Physics, Optoelectronics and Energy & Collaborative Innovation Center of Suzhou Nano Science and Technology, Soochow University, Suzhou, 215006, People's Republic of China
[2] Key Lab of Advanced Optical Manufacturing Technologies of Jiangsu Province & Key Lab of Modern Optical Technologies of Education Ministry of China, Soochow University, Suzhou, 215006, People's Republic of China
[3] State Key Laboratory of Applied Optics, Changchun Institute of Optics, Fine Mechanics and Physics, Chinese Academy of Sciences, Changchun, 130033, People's Republic of China

E-mail: lschen@suda.edu.cn

Received 19 April 2015, revised 15 July 2015
Accepted for publication 27 July 2015
Published 24 August 2015

Abstract

The effects of monomer functionality on performances of holographic polymer dispersed liquid crystal (HPDLC) transmission gratings are systematically investigated. Acrylate monomers with an average functionality ranging from 2.0 to 5.0 are used to prepare these samples. We find scaffolding morphologic transmission gratings (characterized by a high phase separation degree, a well alignment of LCs and low scattering loss) can be obtained irrespective of the monomer functionality, although the exact optimal curing intensity varies. The temporal evolution of the grating formation is studied and the onset time of the LC phase separation decreases significantly with the increase in average monomer functionality. It is also shown that the gratings prepared from low average functionality monomers require a comparatively low switch-off electric field (~8 V μm^{-1}) whilst suffering from mechanical fragility and long-term instability. Our results not only provide a complete understanding of scaffolding morphologic gratings in terms of the material composition effect, but also provide insight into the formation mechanisms of non-droplet morphologic HPDLC gratings.

Keywords: holographic polymer dispersed liquid crystals, Bragg gratings, thin films

(Some figures may appear in colour only in the online journal)

1. Introduction

In the present, the fast expanding market of consumer electronics is revolutionizing our daily life and providing both new challenges and opportunities to scientific and industry researchers in twofold aspects: portability and multi-function. Portability means the devices should be light-weight, at a low manufacturing cost, flexible, and even wearable. While multi-function means our daily consumer electronics (like the mobile phone) should not limit their use to communication and entertainment, but also engage in bio-sensing, environmental monitoring or other fields. Under these considerations, the introduction of flexible photonic integrated circuits (PICs) [1] into the consumer electronics may be of extreme importance. On one hand, flexible PICs naturally fulfill the requirement of portability, and on the other hand, they provide new perspectives into functions, such as evanescent optical sensing, optical communication and spectroscopic analyzing.

Holographic polymer dispersed liquid crystals (HPDLC) gratings are micro-nano structures with attractive optical, mechanical and electrical properties. They have already been demonstrated as biomolecule detectors [2, 3], display devices [4], organic lasers [5–11], optically switchable Bragg gratings [12, 13], switchable optical phase modulators [14], switchable lenses [15], and humidity sensors [16]. Thus, HPDLC gratings deserve renewed research interest as important functional optical components in flexible PICs aimed at consumer electronics.

HPDLC gratings are formed by the anisotropic phase separation of liquid crystals (LCs) from the solid polymer matrix induced by free-radical initiated photo-polymerization [17]. The interference pattern created by two or multiple coherent laser beams is used to irradiate the prepolymer syrup which mainly contains photo-sensitive monomers and LCs. After a set of chemical–physical processes including polymerization, diffusion and phase separation, periodic lamellas with alternating polymer layers and LC layers corresponding to bright regions and dark regions of the interference pattern can be obtained. Although the HPDLC technique can be classified as a variant of the interferometric lithography except that the photo-resist is replaced with the prepolymer mixture, it enjoys two distinct advantages: first, it represents a convenient fabrication technique in which the exposure and development of the grating can be completed in one step; second, the built-in LCs in these gratings are electrically active. As the orientation of LC molecules can be controlled by external electric field, the refractive index contrast and the corresponding optical properties of the periodic structures can be modulated. The latter offers a bridge between electrical circuits and optical functions and is a certification demonstrating the potential for consumer electronics via the flexible PCIs.

As the driving force for the formation of HPDLC gratings is given through the anisotropic depletion of monomers, it is of paramount importance to optimize diffractive properties, electrical response and morphology through the control of the photo-polymerization rate [18, 19]. Average monomer functionality quantifies the number of double bonds of each monomer that could be linked together, which is an important parameter in terms of polymerization rate and density of resulting polymer. Accordingly, there has already been a number of papers analyzing the effect of monomer functionality on the performance of HPDLC gratings. However, conflicting results are often given which make this question even more complicated. Shin *et al* [20] showed that a high-functionality oligomer gives better LC phase separation, due to the immiscibility between LCs and polymer as a result of high crosslink density. Ramsey *et al* [21] found the diffraction efficiency increases monotonously with the acrylate monomer functionality in He–Ne laser cured HPDLC transmission gratings, attributing to the high diffusion rate of LCs. Peng *et al* [22] showed the diffraction efficiency increases with the increase in the loading of a high functionality monomer and hence the average functionality. They attributed the improvement to the low viscosity of the monomer which gives LCs sufficient time to diffuse out before the gelation happens. White *et al* [23, 24] also demonstrated that increasing the monomer functionality improves the diffraction efficiency of HPDLCs, as the increased rate of polymerization reduces the LC droplet size. On the other hand, Park and Kim [25] found an intermediate acrylate monomer functionality of 3 gives the highest diffraction efficiency: at lower functionality, the hooping force induced by the slow polymerization rate is insufficient to squeeze the LC molecules out of the polymer-rich domains; while at higher functionality, the polymerization rate is too fast and most of LCs are entrapped in the polymer-rich domains before efficient diffusion takes place. However, Bensaid *et al* [26] showed that HPDLC gratings prepared from acrylate monomers with a low functionality of 2 can also exhibit efficient diffraction efficiency and phase separation. The most astonishing results were reported by Sarkar *et al* [27]. The authors found that the HPDLC grating morphology is sensitively dependent on the acrylate monomer functionality. The LC droplet size decreases with the decrease in average functionality. Non-droplet morphology gratings can be obtained when the average functionality is 1.5 and the corresponding diffraction efficiency is the highest. Although the conflict of previous results can be partly attributed to the properties of different material compositions and the complexness of the chemical–physical reaction, two important points are often neglected in these studies. (1) By simply changing the monomer functionality whilst the curing conditions staying the same, yhe difference in electro-optical properties of resulting gratings may be attributed to the difference in grating morphology or to the un-optimized curing conditions, instead of the monomer functionality; (2) Characterization of grating properties is overdependent upon the diffraction efficiency. The Bragg diffraction efficiency changes sinusoidally with LC cell thickness, LC phase separation and the orientation of LCs. The refractive index over-modulation phenomenon has often be observed [19], and the 100% diffraction efficiency can be regarded as an optimum combination of the refractive index modulation and cell thickness, but not a better phase separated HPDLC grating.

LCs in scaffolding morphologic HPDLC transmission gratings exist in the form of pure slices instead of droplets [28]. They are homogeneously aligned along the grating vector due to the anchoring force of numerous traverse polymer filaments. Previously, we have presented a detail characterization of the optical properties of the scaffolding morphologic HPDLC grating [29]. The grating exhibits high diffraction efficiency, high LC phase separation degree, low scattering and high polarization dependence. In this work, the effects of monomer functionality on performances of scaffolding morphologic HPDLC transmission gratings are investigated. The average acrylate monomer functionality is varied between 2.0 and 5.0. The curing conditions are optimized in each case and the scaffolding morphologic grating can be prepared irrespective of the monomer functionality. The onset time of phase separation decreases from 156 s to 9 s when the monomer functionality increases from 2.0 to 5.0, indicating a much faster polymerization rate. Birefringence measurement is used to accurately determine the LC phase separation degree which shows a slightly higher phase separation degree at lower functionality. Due to the loose polymer matrix resulting from the

low functionality monomer, these gratings operate at a lower switching electric field and suffer from mechanical fragility. The significant influence of the grating pitch on optimum curing conditions and corresponding phase separation degree is also studied.

2. Experimental part

2.1. Materials

Acrylate monomers used in this study include phthalic diglycol diacrylate (PDDA, Xiyachem) and dipentaerythritol hydroxyl pentaacrylate (DPHPA, Sigma-Aldrich). The chemical structures for the two kinds of monomers are shown in figure 1. Samples with monomer functionality of 2.0, 3.5 and 5.0 can be obtained using pure PDDA, the mixture of PDDA and DPHPA at a molar ratio of 1:1, pure DPHPA, respectively. The standard monomer mixtures also contain 0.5 wt% of the photoinitiator Rose Bengal (RB, Sigma-Aldrich), 1.5 wt% of the coinitiator N-phenyglycine (NPG, Sigma-Aldrich), and 15 wt% of the solubilizer N-vinylpyrrolidone (NVP, Sigma-Aldrich). The monomer mixtures were homogeneously blended for 24 h under dark conditions. Refractive indices for the liquid and cured monomer mixtures were measured by an Abbe Refractometer and are shown in table 1. The refractive index of the cured monomer mixture undergoes a slight increase of 0.03–0.04 due to the reduction in volume after polymerization. The refractive index of the pure polymer decreases slightly with the reduction in monomer functionality, and it matches well with common refractive index of LCs (n_0 = 1.522) at low monomer functionality. In the rest of the paper, these samples are referred to as sample 1, sample 2 and sample 3, in sequence.

2.2. Grating fabrication

For the fabrication of HPDLC gratings, each isotropic monomer mixture was further mixed with 30 wt% of liquid crystal TEB30A (n_0 = 1.522, Δn = 0.17, Silichem). A drop of the prepolymer mixture was then placed between two indium-tin oxide (ITO) coated glass slides separated by 4 μm glass spacers by capillary attraction. The experimental setup for grating fabrication and simultaneous monitoring of the diffractive properties is shown in figure 2. Lasing at 532 nm from a continuous wave Nd: YAG laser is split into two beams (s polarized) after being spatially filtered and collimated. They are then directed symmetrically upon the cell surface from the same side to write the transmission grating. The grating period can be precisely calculated using $\Lambda=\lambda_w/2\ \sin(\theta/2)$, where θ is the intersection angle between the two beams and can be controlled within an error of 0.02°. The intersection angle was first set to be 40° which yields a grating period of 778 nm. The Q factor of these gratings is calculated to be around 15 for visible wavelengths. As the value of Q factor is higher than 1, these gratings work in the Bragg regime. An unpolarized He–Ne laser at 633 nm is incident onto the sample from the other side of the cell at the Bragg angle. As its wavelength falls out of the absorption spectrum of the photo-initiator, the monitoring beam causes negligible influence to the formation of the grating. Prior to being detected, the diffracted probe beam is separated into S- and P-polarization components by a polarizing beam splitter. Each signal is monitored on a separate channel of a photo detector and a computer collects complete signals at intervals of 500 ms. The measured diffraction efficiency for each polarization was defined as $\eta_{s/p} = \frac{I_{s/p}^{1^{th}}}{I_{s/p}^{total}}$, where $I_{s/p}^{1^{th}}$ is intensity of first-order diffraction for each polarization during the grating formation and $I_{s/p}^{total}$ is the intensity of total transmitted light through the sample for each polarization before the curing of the grating.

2.3. Characterizations

Phase separation degree β is defined as the volume ratio of phase-separated LCs to total LCs. Compared with the grating diffraction efficiency, β is a more objective parameter indicating the efficiency of LC phase separation. In common droplet-morphologic HPDLC gratings where LCs phase separates to form independent domains, it is very difficult to accurately determine the value of β, due to the non-uniformity in LC droplet size and shape distribution and the uncertainty about LC director configuration in each droplet [30]. As for the scaffolding morphologic grating, the situation is neat and simple in two ways: (1) phase separated LCs form homogeneous layers and merely scattering loss arises when light is propagating through the grating; (2) LC molecules are well aligned along the grating vector. Based on these two foundations, we have proposed the accurate determination of β through the measurement of average birefringence of the grating [29]. The experimental setup is shown in figure 3. The HPDLC grating is placed between two polarizers P1 and P2 with their transmission axis being orthogonally aligned and a He–Ne laser beam at 633 nm (beam diameter 1.5 mm) used as the incident beam. The laser beam was directed upon the HPDLC grating to the surface normal. As the incident angle is away from the grating Bragg angle, the first order diffraction efficiency is below 1% and almost all the light intensity is transmitted through the sample. The well-aligned phase-separated LC molecules bring a birefringence to the sample. The phase retardation resulting from the birefringence can be deduced from the transmitted light intensity and the amount of phase separated LC can thus be determined. The angle between the grating vector and the transmission axis of either polarizer is set to be 45° for accuracy. We have:

$$\beta = \frac{\lambda_{He-Ne}\ \arcsin\sqrt{\frac{I_T}{I_{OT}}}}{\pi\varphi_{LC\_total}\Delta n_{LC\_bulk}L} \tag{1}$$

where λ_{He-Ne} is the wavelength of incident light, φ_{LC_total} is the volume concentration of LC in the initial prepolymer syrup, L is the cell gap, Δn_{LC_bulk} is the birefringence of bulk nematic LC provided by the manufacturer, I_{OT} is the total light intensity transmitted through the sample (measured before

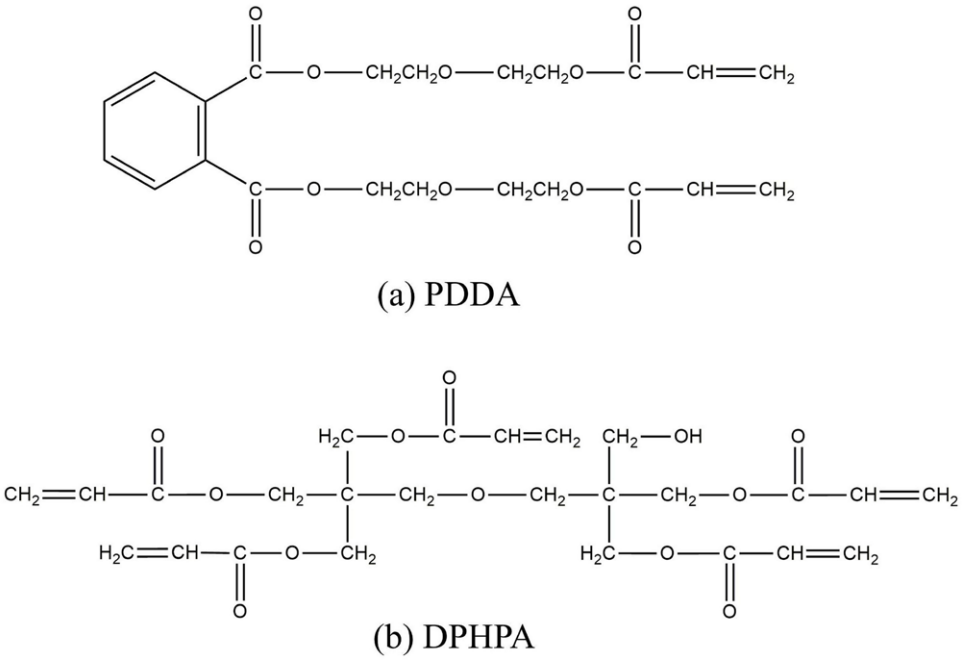

Figure 1. Chemical structures of the acrylate monomers.

Table 1. Refractive index (RI) of pure polymer for different functionality.

Monomer	Average functionality	RI of liquid monomer mixture	RI of cured polymer
PDDA	2.0	1.486	1.526
PDDA + DPHPA	3.5	1.495	1.532
DPHPA	5.0	1.504	1.535

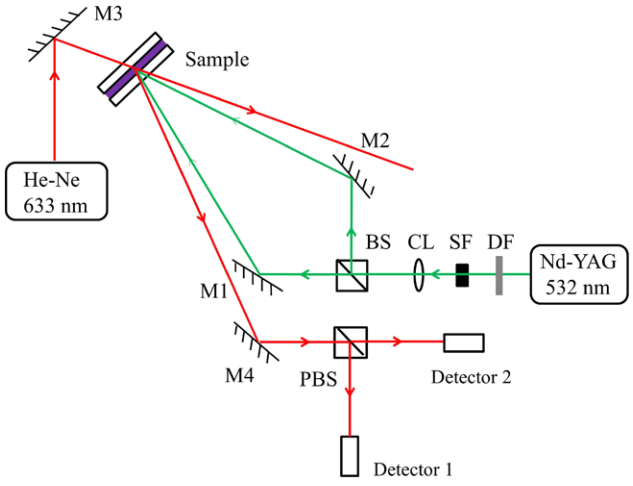

Figure 2. Schematic diagram of the experiment.

P2), and I_T is light intensity through the two orthogonally aligned polarizers.

An atomic force microscopy (AFM) (Nanoscope III) was employed to analyze the surface topology of the transmission gratings. In preparation for AFM analysis, the samples were disassembled by hand and rinsed in alcohol for several minutes to remove the LC. In this way, the initial phase grating composed of alternating layers of LC and polymer transforms into the relief grating which is suitable for AFM measurement. The electro-optical performance of the HPDLC gratings was determined by probing the HPDLC cells with the P polarized He–Ne laser beam. An adjustable power supply was used to provide an electric field (1 kHz frequency) across the cell and intensity of the first-order diffracted beam was monitored. All samples were aged for several days before electro-optical investigation in order to ensure that the grating properties were reasonably stable.

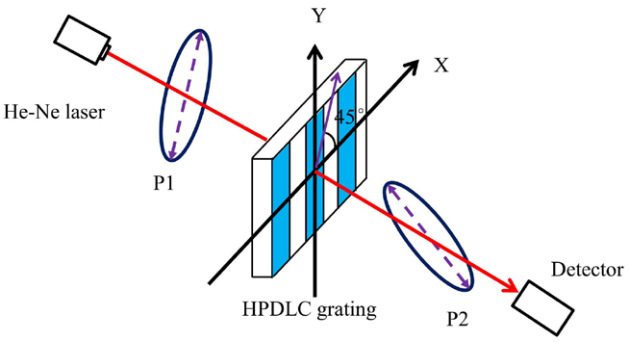

Figure 3. Setup for measuring the LC phase separation degree. P1 and P2 are two orthogonally aligned polarizers. The angle between the grating vector and the transmission axis of either polarizer is 45°.

3. Results and discussions

3.1. Temporal evolution and grating morphology

The temporal evolution of anisotropic HPDLC gratings prepared from monomers with different average functionalities is shown in figure 4. Diffraction efficiencies for both polarizations are normalized for a clear presentation of the results. Two interesting regimes are apparent in each case. When the

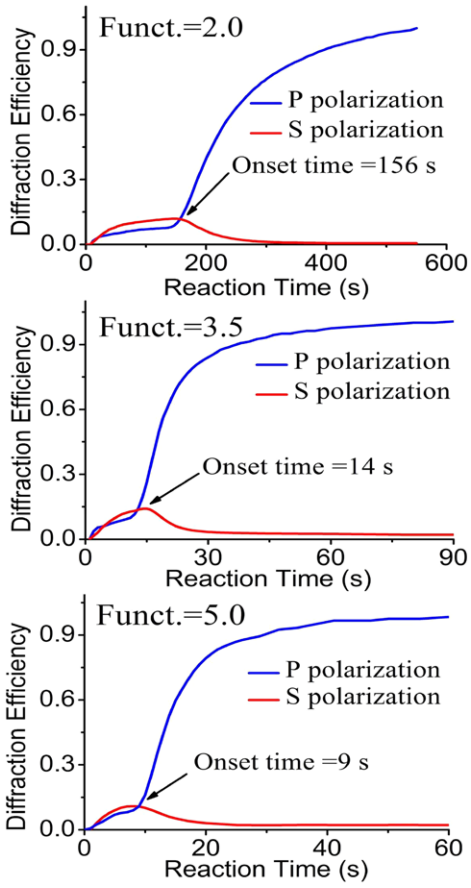

Figure 4. The evolution of diffraction efficiencies for both polarizations during the grating formation for different monomer functionalities.

shutter opens, the diffracted signal for both S polarization and P polarization immediately appears and begins to increase at a moderate rate. This can be attributed to the isotropic grating at the initial stage. This grating forms because the initial LC molecules diffusing into dark regions are miscible with monomers. As rod-like LC molecules are spaced by 'round' monomers, they are isotropically distributed. Refractive index modulation comes from the refractive index difference between isotropic LC molecules and the polymer matrix. According to diffractive equations for an isotropic grating, the ratio of η_p to η_s is $\cos(2\theta_B)$ with θ_B being the Bragg angle, thus the diffraction efficiency for S polarization is slightly higher which agrees well with figure 4. We note that Fuh *et al* reported on the observation of two diffraction efficiency peaks during grating formation and they attributed this to the 180° out of phase caused by the thermal grating effect [31]. The result presented here is different as the total diffraction efficiency of the two polarizations increases monotonously. There appears to be an onset time for each curve at which the diffraction efficiency for P polarization begins to increase at a much faster rate while that for S polarization starts to decrease. Note that this onset time is nearly coincidental with the trigger time of phase separation deduced from the occurrence of light scattering [29, 32]. It is when the LCs in the dark regions reach a critical point, that a two-phase HPDLC grating is formed. We interpret this to be a result of the increasing amount of diffused LC molecules and the gelatin of acrylate monomers. The anisotropic grating is due to a macroscopic ordering of LC molecules along the grating vector: P polarization experiences a refractive index close to n_e maximizing the refractive index modulation of the grating while the refractive index difference between LC layer and polymer matrix for S polarization is almost negligible. The characteristic is different from that observed in a droplet morphologic grating in which a significant diffracted signal for S polarization is still present after the LC phase separation [33]. Thus, it can be regarded as an implication for the scaffolding morphologic grating demonstrating the uniform alignment of LC molecules along the grating vector. The final diffraction efficiency for S polarization increases slightly from sample 1 to sample 3, and it is consistent with the refractive index measurement in table 1. It is also remarkable that the onset time for phase separation decreases sharply from 156 s in sample 1 to 14 s in sample 2, and reaches 9 s in sample 3, implying the significant influence of monomer functionality on grating formation dynamics: In low viscosity and low functionality monomer systems, the polymerization rate and density of cross-linked monomers are restricted by availability of functionality on each monomer. There will not be high molecular weight polymer chains at the early stage but a distribution of dimers and oligomers. As a result, the driving force for LC diffusion is weak and the polymer gel requires a lot of time. In this case, the onset time is late and the whole grating completes around 10 min. Note that the late gelatin point indicates a high C=C double bond conversion which has been observed by many researchers [23, 27, 34]. While for high viscosity and high functionality acrylate monomers, each chain initiator on the monomer will act as a reaction center to capture another monomer, leading to a fast polymerization rate. High molecular weight polymer chains are produced at the early stage and they are insoluble with LCs. Thus the onset time is early and the whole grating completes in 40 s. It is not clear here whether LC molecules have enough time for diffusion, or just to be captured in the polymer matrix.

The high optical anisotropy shown in figure 4 indicates a well alignment of LC molecules along the grating. This feature is in contrast to the low optical anisotropy in droplet morphologic HPDLC gratings [35, 36] and implies scaffolding morphology in all three HPDLC samples. It is necessary to analyze the grating surface profile and optical scattering loss afterwards. Figure 5 shows the surface topology of fabricated HPDLC gratings. We found the HPDLC grating in sample 1 suffers from mechanical fragility. Shattered film is formed when the cell was disassembled by hand with some grating debris attaching to the glasses. The rippled film in figure 5(a) also shows the difficulty in preparing the sample for AFM test. The grating period in figure 5(a) also appears to be slightly different from the other two samples due to the rippled morphology. Although the double bond conversion is high in sample 1, the total number of double bonds for cross-linking is limited and the generated polymer matrix is loose. Note that there are some LC domains distributed in polymer channels in figure 5(b). We attribute it to the incomplete removal of LCs when sample 2 was rinsed in alcohol. The surfaces of all

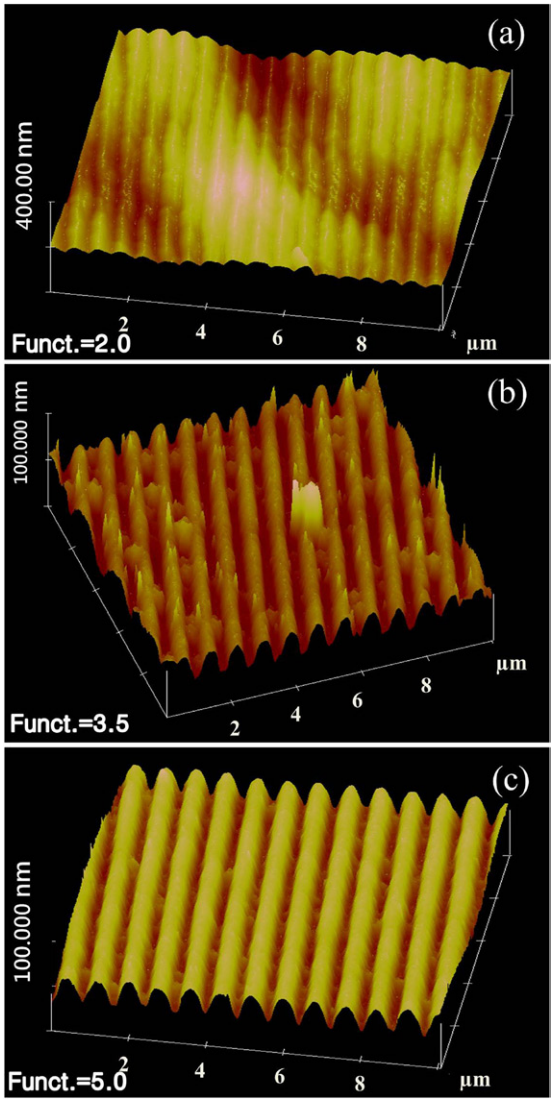

Figure 5. AFM images of transmission gratings prepared from acrylate monomers with different functionality. The measured grating period is around 780 nm.

gratings show sinusoidal profiles. The exact appearance for each grating is slightly different. It can be found that most of the grating surface is very smooth without the presence of irregularities dwelled previously by LC domains [27, 36] indicating the nondroplet-morphology for all samples. In order to measure the scattering loss to further confirm the non-droplet morphology, a He–Ne laser beam was employed to impinge upon the grating to the normal of the cell. By measuring the total input intensity (I_T), the reflected intensity (I_R) and the transmission intensity (I_{Trans}), loss of the grating can be calculated using $\alpha_{loss} = \frac{I_T - I_R - I_{Trans}}{T_T}$. As absorption of the sample at 633 nm is negligible, the loss is caused by scattering domains in these gratings. Scattering loss for S polarization is about 2%, while that for P polarization lies in the range between 4% and 6%. The comparatively higher scattering loss for P polarization agrees with the fact that it experiences a higher refractive index difference. Overall, scattering loss is much lower than that (around 15%) observed in droplet morphologic HPDLC gratings [37, 38], demonstrating the scaffolding morphology in all gratings with average functionality ranging from 2.0 to 5.0.

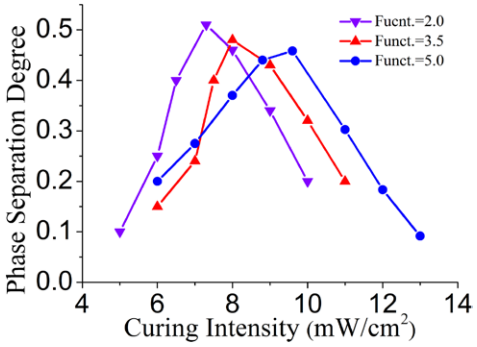

Figure 6. Phase separation degree as a function of curing intensity: down-triangle for sample 1, up-triangle for sample 2 and circle for sample 3.

3.2. Phase separation degree

In the last section, we show a much delayed onset time for phase separation during grating formation with low functionality monomer, and the resulted grating suffers from mechanical fragility due to the loose polymer matrix. While the 'inner properties' of the gratings seem to stay the same: (1) the phase separated LC molecules are well aligned along the grating vector leading to a high optical anisotropy, (2) nondroplet grating morphology with very low scattering loss. There remains a possibility that most LCs are trapped in the polymer matrix in some of these gratings before efficient diffusion takes place, leading to 'fake' samples with very low efficiency. It is then very necessary to characterize the 'efficiency' of these gratings. Note that the birefringence measurement for LC phase separation is valid here due to the uniform alignment of LCs and low scattering loss. In previous studies on the effect of monomer functionality on HPDLC gratings, the curing conditions stay the same and are not optimized for each material system. The change in monomer composition could significantly alter monomer diffusion and polymerization rate properties, and inevitably leads to fluctuations in optimum curing conditions. In consideration of this, the exposure intensity in this study was varied in order to determine the optimum cuing intensity for each sample. The results are shown in figure 6, in which the grating period is 778 nm. There exists an optimum curing intensity for each sample where the LC phase separation reaches a peak. The optimum phase separation degree decreases slightly from 0.52 in sample 1 to 0.45 in sample 3. It seems that the delayed onset time in the gratings fabricated from low functionality monomers allows more time for LC and monomer molecules to diffuse into corresponding regions. Compared with previous studies, these gratings could be classified as efficient, as diffraction efficiencies of 100% are attainable in cells with a thickness around 7 μm. Thus efficient scaffolding morphologic HPDLC gratings have been achieved with monomer functionality ranging from 2.0 to 5.0. Note that the optimum curing intensity is much lower that (over 50 mW cm^{-2}) used in previous papers [36, 39] demonstrating a droplet-like morphology.

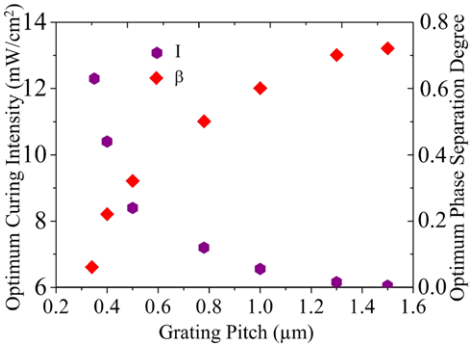

Figure 7. Dependencies of optimum curing intensity and optimum phase separation degree on the grating pitch for sample 1.

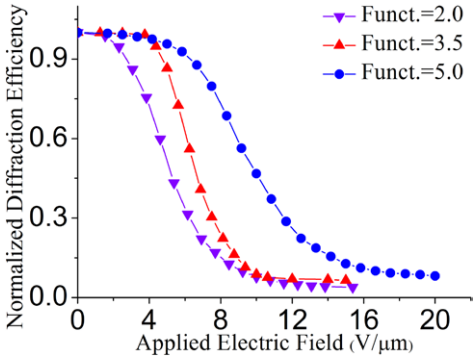

Figure 8. Diffraction efficiency as a function of applied electric field for samples made from different monomer functionalities.

According to the chemical-diffusive model developed by Caputo [40] and Veltri [41], there are two curing regimes for HPDLC grating formation: one is fast curing regime in which the polymerization reaction is very fast and polymer chains grow before efficient monomer diffusion takes place; The other is slow curing regime, in which the polymerization rate is slow and monomers could diffuse across the fringes. The authors also showed nondroplet gratings can be obtained in thiol-ene based HPDLC mixtures by elevating the curing temperature. The accelerated monomer diffusion rate shifts curing from the fast regime to the slow regime. At a first sight, the nondroplet HPDLC gratings in this study can be simply attributed to the weak curing intensity. As the weak curing intensity corresponds to a slow polymerization rate and, thus, the slow curing regime. However, a closer examination of the results presented here reveals some paradoxes: sample 1 with a low monomer viscosity (corresponds to a high monomer diffusion constant) and a low functionality of 2.0 (corresponds to a slow polymerization rate) could result in the nondroplet morphology, while sample 3 with a lower monomer diffusion constant and much faster polymerization rate also result in the nondroplet morphology. A re-examination of the formation parameter B raised by the authors in [41] may provide a more accurate understanding on formation mechanisms: $B = \frac{4\pi D k_t^{1/2}}{(gW_0 I)^{1/2}\Lambda^2}$, where D stands for monomer diffusion constant, k_t is termination constant for the polymerization reaction, $W_0 = I_1 + I_2$ is the total intensity, I is the concentration of initiator, g is the radical generation probability. The exact value of B in each case determines which type of grating is to be formed. It implies that same B values can be obtained with a reduced monomer diffusion constant and increased termination constant. As for radical initiated polymerization, initiators are quenched mainly through chain-radical/chain-radical recombination resulting in deactivated chains. The high functionality monomer has more chains to capture radicals for polymerization and in turn the chain-radical has more probability to quench each other, leading to an increased K_t. In this way, the paradox is solved and the result of efficient nonodroplet morphologic gratings from high functionality monomer is understandable: It is due to the increased termination constant but not due to the polymerization rate.

Figure 7 displays the dependency of optimum curing intensity on the grating pitch for sample 1. Intersection angle between the two curing beams was systematically altered for the required grating period. It is shown that narrower gratings require a stronger curing intensity. It can be partly attributed to the degradation of fringe pattern contrast at a large incident angle. On the other hand, this also shows the influence of the grating pitch on formation dynamics, as narrow periods provide little time for diffusion. It can also be seen from the expression for the parameter B: the grating pitch and curing intensity should be inversely altered in order to keep the value of B a constant. The optimum LC phase separation degree for each grating period is also given in figure 7. Although the curing intensity is optimized for each case, the attainable phase separation degree decreases with the decrease in grating pitch. It is also remarkable that high phase separation degree over 70% can be achieved when the grating period is larger than 1.3 μm, again demonstrating the high efficiency of scaffolding morphologic gratings.

3.3. Switching properties

We show in the last two sections that scaffolding morphologic HPDLC gratings can be obtained with acrylate monomer functionality ranging from 2.0 to 5.0. Although the polymerization rate and onset time for phase separation vary greatly in these samples, they exhibit similar optical properties with high phase separation degree, high optical anisotropy and low scattering loss. It is then necessary to characterize the switching properties. The electro-optical measurements are shown in figure 8. For each of the three gratings, η decreases with increasing amplitude of the electric field, and nature of the electric field dependence varies with the monomer functionality of the composite. When the monomer functionality increases from 2.0 to 5.0, threshold electric field E_{90} increases from 3.1 V μm^{-1} to 7.3 V μm^{-1}, while saturated electric field E_{10} increases from 8.0 V μm^{-1} to 16.0 V μm^{-1}. This numeral means a onefold increase in operation electric field. It has been shown that the anchoring strength of LC molecules in scaffolding morphologic HPDLC gratings depends on the interaction between LC molecules and traversing polymer fibers [28]. It is reasonable that the 'soft' scaffolding branches in loose polymer matrix generated by the low monomer functionality

mixture exert less anchoring strength to LC molecules. Thus these less anchored LC molecules are easy to drive which causes a much decreased switching electric field. We also note that the positive dependence of the required switching field on the monomer functionality is quite different from previous reports. Ramsey *et al* [21] and Peng *et al* [22] found the switch off field decreases with the increase in monomer functionality. They attributed it to the increase phase separation and thus the increased size of the LC droplets, as bigger LC domains are easier to reorient under the electric field. On the other hand, Sarkar *et al* [27] showed the required saturation field undergoes a sudden decrease from 25 $V\mu m^{-1}$ to 12 $V\mu m^{-1}$ with an increase in functionality from 1.2 to 2.0. With a further increase in functionality from 2.0 to 3.5, a slight decrease in the operation field has been observed. The sharp decrease is due to the difference in grating morphology: LC molecules in scaffolding morphologic are strongly bounded by polymer filaments, and they are difficult to drive when compared with LC droplets. While a slight decrease is attributed to the enlargement of LC domain size when the monomer functionality is increased. Thus, the influence of monomer functionality on grating switching properties by previous reports is mainly caused by the difference in morphology, while the effect of monomer functionality is confused. In this paper, the grating morphology stays the same, and the difference in switching properties is caused by the properties of the cured polymer and thus the monomer functionality. It is also interesting to see that the saturation field doubled when the monomer functionality increases from 2.0 to 5.0, demonstrating the importance of material selection with regard to electro-optical properties. An intermediate monomer functionality of 3.5 may be the best choice for the fabrication of scaffolding morphologic HPDLC gratings. Put aside the similar optical properties there three samples share, sample 2 not only requires a comparatively low switching field (E_{10} = 9 $V\mu m^{-1}$), but also is free from mechanical fragility. The competition of a grating in 40 s also eliminates the adverse effects of vibration during the recording process. Note that although the saturation field in this case is still higher than that for droplet morphologic gratings [36], it is comparable with that in polymer liquid-crystal polymer slices gratings [42].

4. Conclusion

In this work, the effect of monomer functionality on the scaffolding morphologic HPDLC gratings is investigated. Monomer functionality is varied from 2.0 to 5.0 and the curing condition is optimized in each case. The onset time for phase separation decreases from 156 s in sample 1 to 9 s in sample 3, indicating an accelerated polymerization rate. By characterizing the optical properties and grating morphology, we show polymer scaffolding morphologic HPDLC gratings can be obtained irrespective of the monomer functionality. It is proposed that nondroplet morphologic gratings can be obtained by either improving the monomer diffusion constant or increasing the termination constant of the polymerization reaction. As for the choice of monomers, an intermediate monomer functionality of 3.5 is preferred. These gratings not only operate at a comparatively low electric field, but also have better mechanical stability.

Acknowledgments

The authors gratefully acknowledge financial support from the Priority Academic Program Development of Jiangsu Higher Education Institutions (PAPD).

References

[1] Hu J, Li L, Lin H, Zhang P, Zhou W and Ma Z 2013 Flexible integrated photonics: where materials, mechanics and optics meet *Opt. Mater. Express* **3** 1313–31
[2] Woltman S J, Jay G D and Crawford G P 2007 Liquid-crystal materials find a new order in biomedical applications *Nat. Mater.* **6** 929–38
[3] Hsiao V K S, Waldeisen J R, Zheng Y, Lloyd P F, Bunning T J and Huang T J 2007 Aminopropyltriethoxysilane (APTES)-functionalized nanoporous polymeric gratings: fabrication and application in biosensing *J. Mater. Chem.* **17** 4896–901
[4] Qi J and Crawford G P 2004 Holographically formed polymer dispersed liquid crystal displays *Displays* **25** 177–86
[5] Jakubiak R, Tondiglia V P, Natarajan L V, Sutherland R L, Lloyd P, Bunning T J and Vaia R A 2005 Dynamic lasing from all-organic 2D photonic crystals *Adv. Mater.* **17** 2807–11
[6] Lucchetta D E, Vita F, Castagna R, Francescangeli O and Simoni F 2012 Laser emission based on first order reflection by novel composite polymeric gratings *Photonics Nanostruct. Fundam. Appl.* **10** 140–45
[7] Huang W, Diao Z, Liu Y, Peng Z, Yang C, Ma J and Xuan L 2012 Distributed feedback polymer laser with an external feedback structure fabricated by holographic polymerization technique *Org. Electron.* **13** 2307–11
[8] Liu Y J, Sun X W, Shum P, Li H P, Mi J and Ji W 2006 Low-threshold and narrow-linewidth lasing from dye-doped holographic polymer-dispersed liquid crystal transmission gratings *Appl. Phys. Lett.* **88** 061107
[9] Lucchetta D E, Criante L, Francescangeli O and Simoni F 2004 Light amplification by dye-doped holographic polymer dispersed liquid crystals *Appl. Phys. Lett.* **84** 4893–95
[10] Lucchetta D E, Criante L, Francescangeli O and Simoni F 2004 Wavelength flipping in laser emission driven by a switchable holographic grating *Appl. Phys. Lett.* **84** 837–39
[11] Li M S, Fuh A Y-G and Wu S-T 2012 Multimode lasing from the microcavity of an octagonal quasi-crystal based on holographic polymer-dispersed liquid crystals *Opt. Lett.* **37** 3249–51
[12] Urbas A, Klosterman J, Tondiglia V, Natarajan L, Sutherland R, Tsutstumi O, Ikeda T and Bunning T 2004 Optical switchable Bragg reflectors *Adv. Mater.* **16** 1453–56
[13] Sutherland R L, Natarajan L V, Tondiglia V P, Siwecki S A, Chandra S and Bunning T J 2001 Switchable holograms for displays and telecommunications *Proc. SPIE* **4463** 1–10
[14] Sio L D, Tabiryan N, Caputo R, Veltri A and Umeton C 2008 Policryps structures as switchable optical phase modulators *Opt. Express* **16** 7619–24
[15] Jashnsaz H, Nataj N H, Mohajerani E and Khabbazi A 2011 All-optical switchable holographic Fresnel lens based on azo-dye-doped polymer-dispersed liquid crystals *Appl. Opt.* **50** 4295–301

[16] Shi J, Hsiao V K S and Huang T J 2007 Nanoporous polymeric transmission gratings for high-speed humidity sensing *Nanotechnology* **18** 465501
[17] Sutherland R L, Natarajan L V and Tondiglia V P 1993 Bragg Gratings in an acrylate polymer consisting of periodic polymer-dispersed liquid-crystal planes *Chem. Mater.* **5** 1533–38
[18] Fuh A Y-G, Chen W-K, Cheng K-T, Liu Y-C, Liu C-K and Chen Y-D 2015 Formation of holographic gratings in polymerdispersed liquid crystals using off-resonant light *Opt. Mater. Express* **5** 774–80
[19] Bunning T J, Natarajan L V, Tondiglia V P and Sutherland R L 2000 Holographic polymer-dispersed liquid crystals (H-PDLCs) *Annu. Rev. Mater. Sci.* **30** 83–115
[20] Shin E Y, Kim E H and Kim B K 2004 Effects of oligomer functionality in holographic polymer dispersed liquid crystal *J. Korean Phys. Soc.* **45** 697–99
[21] Ramsey R A and Sharma S C 2009 Effects of monomer functionality on switchable holographic gratings formed in polymer-dispersed liquid-crystal cells *Chem. Phys. Chem.* **10** 564–70
[22] Peng H, Ni M, Bi S, Liao Y and Xie X 2014 Highly diffractive, reversibly fast responsive gratings formulated through holography *RSC Adv.* **4** 4420–26
[23] White T J, Natarajan L V, Tondiglia V P, Lloyd P F, Bunning T J and Guymon C A 2007 Monomer functionality effects in theformation of thiol-ene holographic polymer dispersedliquid crystals *Macromolecules* **40** 1121–27
[24] White T J, Natarajan L V, Bunning T J and Guymon C A 2007 Contribution of monomer functionality and additives to polymerization kinetics and liquid crystal phase separation in acrylate-based polymer-dispersed liquid crystals (PDLCs) *Liq. Cryst.* **34** 1377–85
[25] Park M S and Kim B K 2006 Transmission holographic gratings produced using networked polyurethane acrylates with various functionalities *Nanotechnology* **17** 2012–17
[26] Bensaid H, Maschke U, Sakhno O and Stumpe J 2009 Highly efficient holographic PDLC based on acrylate monomers with low functionality *Mol. Cryst. Liq. Cryst.* **502** 37–46
[27] Sarkar M D, Gill N L, Whitehead J B and Crawford G P 2003 Effect of monomer functionality on the morphology and performance of the holographic transmission gratings recorded on polymer dispersed liquid crystals *Macromolecules* **36** 630–38
[28] Vardanyan K K, Qi J, Eakin J N, Sarkar M D and Crawford G P 2002 Polymer scaffolding model for holographic polymer-dispersed liquid crystals *Appl. Phys. Lett.* **81** 4736–38
[29] Huang W, Liu Y, Diao Z, Yang C, Yao L, Ma J and Xuan L 2012 Theory and characteristics of holographic polymer dispersed liquid crystal transmission grating with scaffolding morphology *Appl. Opt.* **51** 4013–20
[30] Sutherland R L 2002 Polarization and switching properties of holographic polymer-dispersed liquid-crystal gratings. I. Theoretical model *J. Opt. Soc. Am.* B **19** 2995–3003
[31] Fuh A Y-G, Ko T-C, Tsai M-S, Huang C-Y and Chien L-C 1998 Dynamical studies of gratings formed in polymer-dispersed liquid crystal films *J. Appl. Phys.* **83** 679–83
[32] Sutherland R L, Tondiglia V P and Natarajan L V 2001 Evolution of anisotropic reflection gratings formed in holographic polymer-dispersed liquid crystals *Appl. Phys. Lett.* **79** 1420–22
[33] Harbour S, Kelly J V, Galstian T and Sheridan J T 2007 Optical birefringence and anisotropic scattering in acrylate based holographic polymer dispersed liquid crystals *Opt. Commun.* **278** 28–33
[34] Natarajan L V, Shepherd C K, Brandelik D M, Sutherland R L, Chandra S, Tondiglia V P, Timlin D and Bunning T J 2003 Switchable holographic polymer-dispersed liquid crystal reflection gratings based on thiol-ene photopolymerization *Chem. Mater.* **15** 2477–84
[35] Sutherland R L, Natarajan L V, Tondiglia V P, Chandra S, Shepherd C K, Brandelik D M, Siwecki S A and Bunning T J 2002 Polarization and switching properties of holographic polymer-dispersed liquid-crystal gratings. II. Experimental investigations *J. Opt. Soc. Am.* B **19** 3004–12
[36] Sarkar M D, Qi J and Crawford G P 2002 Influence of partial matrix fluorination on morphology and performance of HPDLC transmission graings *Polymer* **43** 7335–44
[37] Caputo R *et al* 2009 Policryps: a liquid crystal composed nano/microstructure with a wide range of optical and electro-optical applications *J. Opt. A: Pure Appl. Opt.* **11** 024017
[38] Sutherland R L, Natarajan L V, Tondiglia V P, Bunning T J and Adams W W 1994 Electrically switchable volume gratings in polymer-dispersed liquid crystals *Appl. Phys. Lett.* **64** 1074–76
[39] Jazbinšek M, Olenik I D and Zgonik M 2001 Characterization of holographic polymer dispersed liquid crystal transmission gratings *J. Appl. Phys.* **90** 3831–37
[40] Caputo R, Sukhov A V, Tabirian N V, Umeton C and Ushakov R F 2001 Mass transfer processes induced by inhomogeneous photo-polymerisation in a multicomponent medium *Chem. Phys.* **271** 323–35
[41] Veltri A, Caputo R, Umeton C and Sukhov A V 2004 Model for the photoinduced formation of diffraction gratings in liquid-crystalline composite materials *Appl. Phys. Lett.* **84** 3492–94
[42] Caputo R, Trebisacce I, Sio L D and Umeton C P 2011 Phase modulator behavior of a wedge-shaped policryps diffraction grating *Mol. Cryst. Liq. Cryst.* **549** 29–36